




Article

The Potential Therapeutic Role of Green-Synthesized Selenium Nanoparticles Using Carvacrol in Human Breast Cancer MCF-7 Cells

Mohamed S. Othman ^{1,2,*}, Shimaa M. Aboelnaga ¹, Ola A. Habotta ³, Ahmed E. Abdel Moneim ^{4,*}
and Manal M. Hussein ⁴

¹ Basic Sciences Department, Deanship of Preparatory Year, University of Ha'il, Hail 2440, Saudi Arabia

² Faculty of Biotechnology, October University for Modern Science and Arts (MSA), Giza 12566, Egypt

³ Department of Forensic Medicine and Toxicology, Faculty of Veterinary Medicine, Mansoura University, Mansoura 35516, Egypt

⁴ Zoology and Entomology Department, Faculty of Science, Helwan University, Cairo 11795, Egypt

* Correspondence: biostar55@yahoo.com (M.S.O.); ahmed_abdelmoneim@science.helwan.edu.eg (A.E.A.M.)

Abstract: The disadvantages and side effects of currently available breast cancer (BC) therapies have compelled researchers to seek new therapeutic strategies. This study was designed to investigate the effect of selenium nanoparticles biosynthesized with carvacrol (SeNPs-CV) on breast cancer (MCF-7) cell lines and to explore possible underlying pathways. Flow cytometry, MTT assays, and various biochemical techniques were used to evaluate the anti-proliferative effects of SeNPs-CV on MCF-7 cells. Cytotoxicity assays showed that treatment with SeNPs-CV could effectively reduce MCF-7 cell proliferation and viability in a dose-dependent manner. However, SeNPs-CV had no cytotoxic effect against Vero cells. Furthermore, SeNPs-CV showed better anticancer activity than metal nanoparticles of selenium evidenced by the lower IC₅₀ obtained in MCF-7 cells (8.3 µg/mL versus 41.6 µg/mL, respectively). Treatment with SeNPs-CV directly targeted Bcl-2, Bax, and caspase-3, leading to the mitochondrial leakage of cytochrome C and subsequent activation of the apoptotic cascade in MCF-7 cells. In addition, MCF-7 cells treated with SeNPs-CV exhibited elevated levels of oxidative stress, as indicated by noticeable rises in 8-OHdG, ROS, NO, and LPO, paralleled by significant exhaustion in GSH levels and antioxidant enzymes activity. In addition, the administration of SeNPs-CV induced the inflammatory mediator IL-1β and downregulated the expression of cell-proliferating nuclear antigen (PCNA) in MCF-7 cells, which plays a critical role in apoptosis. Therefore, the ability of SeNPs-CV to fight BC may be due to its ability to induce oxidative stress, inflammation, and apoptosis in tumor cells. These findings demonstrate the therapeutic potential of Se nanoparticles conjugated with CV, which may provide a novel approach for combination chemotherapy in BC.

Keywords: selenium nanoparticles; carvacrol; MCF-7 cells; apoptosis; cell; oxidative stress; proliferating cell nuclear antigen



Citation: Othman, M.S.; Aboelnaga, S.M.; Habotta, O.A.; Moneim, A.E.A.; Hussein, M.M. The Potential Therapeutic Role of Green-Synthesized Selenium Nanoparticles Using Carvacrol in Human Breast Cancer MCF-7 Cells. *Appl. Sci.* **2023**, *13*, 7039. <https://doi.org/10.3390/app13127039>

Academic Editors: Juliet Sackey and Bertrand Sone

Received: 5 May 2023

Revised: 6 June 2023

Accepted: 9 June 2023

Published: 12 June 2023



Copyright: © 2023 by the authors. Licensee MDPI, Basel, Switzerland. This article is an open access article distributed under the terms and conditions of the Creative Commons Attribution (CC BY) license (<https://creativecommons.org/licenses/by/4.0/>).

1. Introduction

Breast cancer (BC) is the second most common cancer type overall and the most common cancer in women. Every year, there are more than two million new instances of BC, which results in 42,000 fatalities. Breast cancer patients' extended survival rates following surgery or chemotherapy treatments are still appalling due to the substantial chances of recurrence and metastasis [1]. Chemotherapy is the highly effective and widely used treatment for a variety of malignancies, including BC. There are already over a hundred nonspecific targeting anti-tumor medications already available; nevertheless, their use is accompanied with a number of adverse responses that might result in mortality [2]. Nonetheless, the unfavorable rates of curing and survival for patients

with BC necessitate increased efforts to develop new strategies for treating BC, and the discovery of a novel, safe, and effective drug for the treatment of BC is urgently required.

Natural NPs are thought to be appealing for the development of theragnostic systems. Multifunctional and multivalent nanostructures can be constructed using an interdisciplinary approach in order to develop unique and effective cancer therapeutics. Specifically, several of the nanocarriers addressed have claimed to be capable of encapsulating and co-delivering imaging moieties, medicines, and genes, as well as detecting cancer cells by attaching to certain receptors. Complex natural-based nanoparticulated formulations may thus contain the key to effective cancer care [3,4].

Many studies have recently shown that naturally occurring terpenoids can be employed in therapeutic applications and that a diet high in terpenoids is inversely associated with the risk of chronic illnesses such as cancer [5,6]. Terpenoids are a class of organic compounds found in various medicinal plants. Some terpenoids are structurally related to human hormones [7]. Carvacrol (5-isopropyl-2-methylphenol) is a member of the monoterpene phenols and is present in many aromatic plants including *Origanum vulgare*, *Satureja hortensis*, *Thymus vulgaris*, *Thymbra capitata*, *Origanum dictamnus*, *Satureja montana*, *Origanum majorana*, and *Thymus serpyllum* [8]. Carvacrol (CV) has been authorized for use as a safe food flavoring, additive, and preservative by the Federal Drug Administration and is generally regarded as safe for eating [9]. Carvacrol is further used as a scent in cosmetics [10]. Many investigations have proven CV's biological effects and therapeutic potential as clinically significant. In vitro and in vivo research has revealed numerous pharmacological characteristics of CV such as anti-mutagenic, analgesic, anti-microbial, anti-tumor, anti-parasitic, and anti-oxidant activity [10,11]. Additionally, CV-rich essential oils have potent antioxidant activities comparable to those of vitamin E and ascorbic acid [12]. Meanwhile, several prior studies have revealed that CV exhibits a variety of cytotoxic and anticancer effects. It has been shown to prevent the proliferation of human erythroleukemic K562 and A549 non-small lung cancer cells [6]. Yet, the mechanism behind its anti-cancer action has not yet been identified [13].

Selenium (Se) is a crucial micronutrient needed for many vital biological activities [3]. Increasing interest is being paid to the use of selenium nanoparticles (SeNPs) as anti-cancer agents or as nano carriers of drugs for cancer therapy due to their superior anticancer efficacies, biocompatibility, and reduced toxicity compared to inorganic or organic selenium compounds. Supporting this hypothesis, many studies have reported that SeNPs have shown promising results in the treatment of a number of malignancies, including prostate cell cancer, glioma lung cancer, melanoma, and breast cancer. The key strategy by which SeNPs combat cancer is the stimulation of apoptotic pathways [14].

Nowadays, combinatorial nanomedicine has evolved into an attractive strategy that provides several potential alternatives for multi-targeted chemotherapy, particularly in the field of resistant cancers such as BC [15]. Furthermore, SeNPs may be excellent drug delivery nanocarriers due to their high cellular absorption rates by diverse cell types [3]. Green synthesis, which uses plant-derived phytochemicals as reducing and capping agents, is a cheaper and less hazardous method for synthesizing nanoparticles [4]. Additionally, these phytochemicals can support different medicinal applications due to their antioxidant, anti-cancer, and anti-inflammatory activities [16]. To the best of our knowledge, the anticancer efficacy of CV in combination with Se-NPs has not yet been examined. Therefore, this study sought to employ CV as an environmentally friendly substance in the preparation of SeNPs, while also utilizing SeNPs as a carrier for CV to increase its bioavailability and penetration power into cancer cells. In addition, this study evaluates the antitumor potential of the SeNPs-CV combination in the breast cancer (MCF-7) cell lines and identifies underlying mechanisms of their anti-proliferative action. The results of this study provide new insights that point to SeNPs-CV as a promising combination in BC therapies.

2. Materials and Methods

2.1. Chemicals and Reagents

Sigma-Aldrich (St. Louis, MO, USA) provided the CV (CAS Number: 499-75-2), cisplatin, and sodium selenite. The reagents used were of the highest analytical quality unless otherwise specified. Deionized distilled water (ddH₂O) was employed as a solvent for selenium, whilst dimethyl sulfoxide (DMSO; Sigma-Aldrich, USA) was used to generate the principal stock solutions of CV and SeNPs-CV at a concentration of 10 mg/mL and stored at −20 °C until use.

2.2. Synthesis and Characterization of SeNPs-CV

A total of 5 mL of CV (10 mg/mL) was added drop wise to 5 mL (10 mg/mL) Na₂SeO₃ and was stirred for 24 h at 37 °C. The reaction mixture was periodically examined for any color changes and subjected to a UV-Vis spectrophotometer analysis. The produced SeNPs were collected by centrifuging the reaction mixture at 1500× *g* after the completion of the reaction. A Zetasizer was used to examine the SeNPs-CV's size. Fourier transform infrared spectroscopy was used to determine the molecular constitution of SeNPs (FTIR; PerkinElmer, Hopkinton, MA, USA). Moreover, transmission electron microscopy was used to describe the morphology of SeNPs-CV (TEM, JEOL Ltd., Tokyo, Japan). Imaging was done at a 100 kV accelerating voltage after a drop of nanoparticle solution was put on a copper mesh that had been coated with carbon. Metal nanoparticles of selenium (SeNPs) were synthesized based on the previous study of our research group [17]. Briefly, sodium selenite was reduced with glutathione in the presence of bovine serum albumin (BSA) and the size of the obtained NPs was in the range of 10 to 80 nm.

2.3. Cell Line and Culture Condition

As a first step, the cells supplied by VACSERA (Giza, Egypt) were grown in Dulbecco's Modified Eagle's Medium (DMEM) (Sigma-Aldrich, Inc.) supplemented with 10% heat-inactivated FBS, 4 mM glutamine, 100 IU/mL streptomycin, and penicillin. The cells were kept in a 5% CO₂ incubator. The medium was changed every 48 h until the growth reached 80% confluence, and then the exponential growing cells were used for all conducted experiments.

2.4. MTT Assay

The cytotoxicity of CV, SeNPs, SeNPs-CV, and CP was determined by MTT as described previously by Van Meerloo et al. [18]. MCF-7 or Vero cells (1 × 10⁴ cells/mL) were cultured in the specific plates and were separately incubated with different doses of CV, SeNPs, SeNPs-CV, and CP for 24 h at 37 °C in a humidified atmosphere of 5% CO₂. Following a PBS wash, the cells were treated with 20 µL of MTT (Invitrogen, Thermo Scientific, Karlsruhe, Germany; 5 mg/mL) at 37 °C. Following treatment for 30 min, the formed formazan crystals were immersed in 200 µL of DMSO and incubated once again for 30 min at 37 °C. The intensity of the dark blue color was measured using a microplate reader (Bio-Rad Company, CA, USA) at 570 nm. Meanwhile, the vehicle-treated group was administrated only with 0.1% DMSO. After the identification of half-maximal inhibitory concentrations (IC₅₀s), half of the IC₅₀s of CV, SeNPs, SeNPs-CV, and CP were used to measure the antitumor potential of these compounds.

2.5. Determination of Cell Death by Flow Cytometry

Following the manufacturer's instructions, a commercial kit (Bioscience, CA, USA) was used to determine the proportional amount of cell death caused by apoptosis or necrosis. Briefly, MCF-7 were treated for 24 h with CV, SeNPs-CV or CP, then the cells were then stained with Annexin V conjugated with fluorescein isothiocyanate (FITC) and propidium iodide (PI) and subsequently analyzed by flow cytometry (Cytomics FC500-MPL). Cells positive for Annexin V-FITC but negative for PI were considered as early apoptotic cells,

while double positive cells were considered late apoptotic cells. Cells that were positive only for PI staining were identified as necrotic cells.

2.6. Apoptosis Markers Determination

ELISA kits (Abcam, Cambridge, UK) were used to determine apoptotic markers (Bcl-2, Bax, caspase-3, and cytochrome c proteins) according to the manufacturer's protocols. At 405 nm, the produced color was quantified with a microplate reader (Biotech, Inc., Alpharetta, GA, USA).

2.7. Molecular Assay for Assessing the Expression Level of Proliferating Cell Nuclear Antigen (PCNA)

Real-time PCR was operated to identify the expression rate of the PCNA gene. TRIzol reagent (Life Technologies, Malvern, PA, USA) was used to separate total RNA from MCF-7 cells, and cDNA was generated using RevertAid™ (Life Technologies, Malvern, PA, USA) (Fermentas, Thermo Fisher Scientific, Chino, CA, USA). mRNA levels were determined using the SYBR Green PCR kit (Qiagen, Germantown, MD, Germany). Quantitative PCR was done using a ViiATM 7 PCR machine (Applied Biosystems, Waltham, MA, USA), with β -actin as the housekeeping gene for all data standards. The qPCR primers' sequences were as follows:

PCNA F: 5'-GCCAGAGCTCTTCCCTTACG-3',
R: 5'-TAGCTGGTTTCGGCTTCAGG-3'.
 β -actin F: 5'-GTCATTCAAATATGAGATGCGT-3'
R: 5'-GCTATCACCTCCCCTGTGTG-3'.

2.8. Assessment of Oxidative Stress Markers

MCF-7 cells (2×10^5 cell/mL) were exposed to CP, CV, and SeNPs-CV for 24 h. Cells were lysed in a buffer after harvesting, and the lysate was centrifuged at $12,000 \times g$ for 1 min at 4 °C, and the supernatant was collected and utilized to identify ROS levels using the DCFH-DA, as described in our previous work [19]. Furthermore, lipid peroxidation (LPO) and nitric oxide (NO) were measured using the colorimetric methods reported by Ohkawa et al. [20] and Green et al. [21], respectively. Meanwhile, the 8-hydroxy-2-deoxyguanosine (8-OHDG) level was detected with ELISA techniques (ELISAKITS. CO., London, UK) according to the manufacturer's protocol and the final color was read at a microplate reader at 420 nm (Biotech, Inc., Alpharetta, GA, USA).

2.9. Determination of the Antioxidant Markers

Catalase (CAT) activity has been measured based on the rate of H_2O_2 decomposition at 240 nm according to Aebi [22]. Superoxide dismutase (SOD) activity was identified at 560 nm, as described by Misra and Fridovich [23], based on its ability to prevent the reduction of nitroblue tetrazolium (NBT) to blue-colored formazan in the presence of phenazine methosulfate (PMS) and NADH. The activity of glutathione peroxidase (GPx) was measured using the Tappel [24] method. GPx accelerates the breakdown of GSH, causing the absorbance at 340 nm to decrease, which is directly related to GPx activity. Meanwhile, the GSH level was evaluated using Ellman's reagent [25].

2.10. Evaluation of Interleukin-1 Beta (IL-1 β)

R&D Systems' (Minneapolis, MN, USA) ELISA kits were used to evaluate the levels of inflammatory cytokine IL-1 β according to the manufacturer's guidelines using microplate reader (Biotech, Inc., Alpharetta, GA, USA).

2.11. Statistical Analysis

All data are expressed in terms of the mean and standard deviation (SD). To compare more than two groups, one-way ANOVA and post hoc Duncan's test were used. The

statistical program SPSS (20.0) was used for the analysis. Significant differences were taken into consideration if p values were less than 0.05.

3. Results

3.1. SeNPs-CV Particles' Characterization

The green synthesis of SeNPs was confirmed by the transformation of the reaction mixture from clear to deep ruby red. SeNPs-CV had a mean diameter of 134.7 nm and a mean zeta potential of -26.8 mV (Figure 1A,B). The particle size distribution of the selenium nanoparticles was determined by the polydispersity index (PDI), and PDI was found to be 0.48, suggesting homogeneity and a uniform dispersion of SeNPs. These results are in agreement with Shahabadi et al. [26] who found that the green-synthesized SeNPs have an average size of 146 nm with a low PDI of 0.521. The morphology of SeNPs-CV was observed by TEM (Figure 1E). The nanoparticles displayed a spherical shape with a particle size less than 200 nm, confirming the Zetasizer findings. The FT-IR spectrum of artificially produced SeNPs-CV and CV alone is shown in Figure 1C,D: the O-H group is represented by a wide peak at 3326.70 cm^{-1} with a slight downshift from 3338.31 cm^{-1} that presented in CV; the branched alkane CEC stretching band can be seen at 2137.65 cm^{-1} ; and the C=C stretching band at 1635.07 cm^{-1} . These two bands are modified bands at 2127.39 cm^{-1} and 1638.21 cm^{-1} of CV. A new band at 455.41 cm^{-1} is present due to C-X stretch carbon compounds with Se, as an indicator of a successful preparation process and conjugation between Se and CV. These findings point to the presence of several functional groups that could be responsible for the reduction and stability of SeNPs-CV.

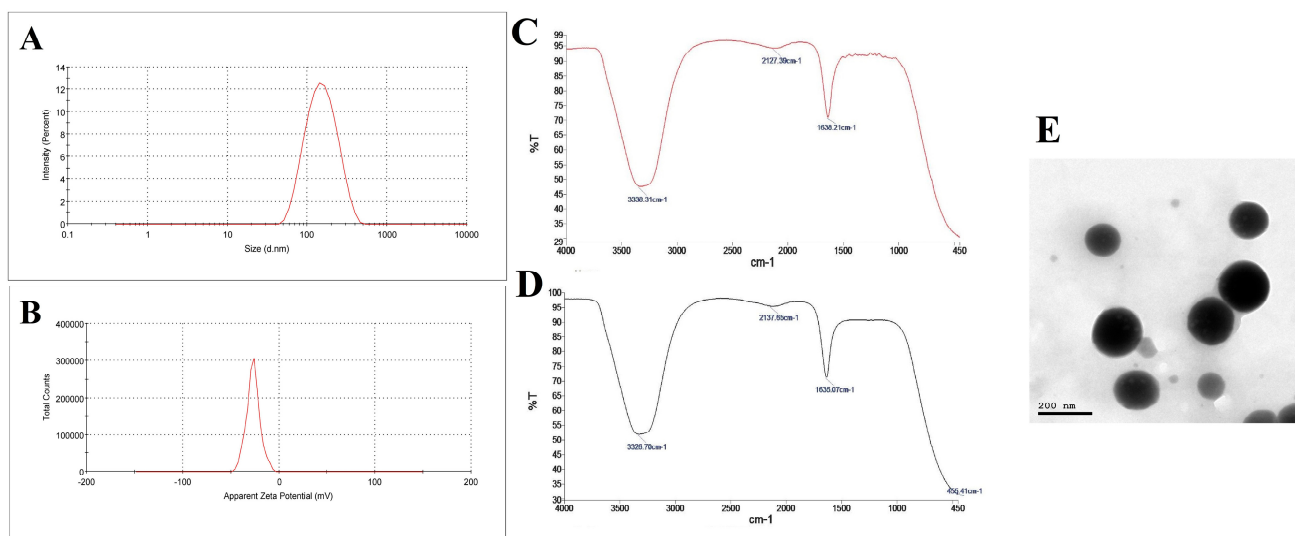


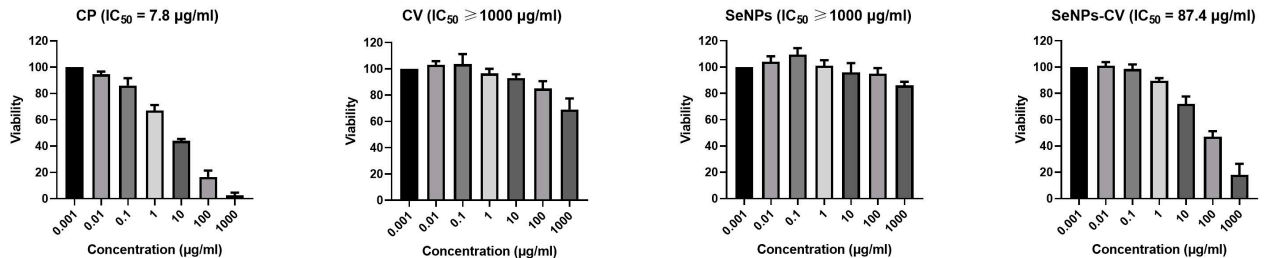
Figure 1. Characters of green-synthesized SeNPs using carvacrol. (A) Hydrodynamic diameter of green-synthesized SeNPs using carvacrol as determined by Zetasizer. (B) Zeta potential of green-synthesized SeNPs using carvacrol as assessed by Zetasizer. (C) FTIR spectra of carvacrol. (D) FTIR spectra of green-synthesized SeNPs using carvacrol. (E) TEM image of green-synthesized SeNPs using carvacrol.

3.2. Cytotoxic Effect and Growth Inhibition of SeNPs-CV

To assess the cytotoxic effects of SeNPs-CV against MCF-7 cells, CV, SeNPs, SeNPs-CV, and cisplatin (a chemotherapeutic drug used as a positive control) were used to treat the cells over a range of concentrations. Cell viability was significantly reduced in a dose-dependent manner in the treated groups in contrast to the vehicle group (0 μM ; Figure 2). The IC_{50} values for CP, CV, SeNPs, and SeNPs-CV in MCF-7 cells were 1.9 $\mu\text{g/mL}$, 32.1 $\mu\text{g/mL}$, 41.6 $\mu\text{g/mL}$, and 8.3 $\mu\text{g/mL}$, respectively. According to these results, the cytotoxicity of the combination of SeNPs-CV in MCF-7 cells was higher than that of CV and SeNPs alone. Furthermore, the cytotoxicity of different compounds towards normal

cells was determined using an MTT assay and the data are presented in Figure 2. The IC_{50} values for CP, CV, SeNPs, and SeNPs-CV in MCF-7 cells were 7.8 $\mu\text{g}/\text{mL}$, >1000 $\mu\text{g}/\text{mL}$, >1000 $\mu\text{g}/\text{mL}$, and 87.4 $\mu\text{g}/\text{mL}$, respectively.

Vero Cells



MCF-7 Cells

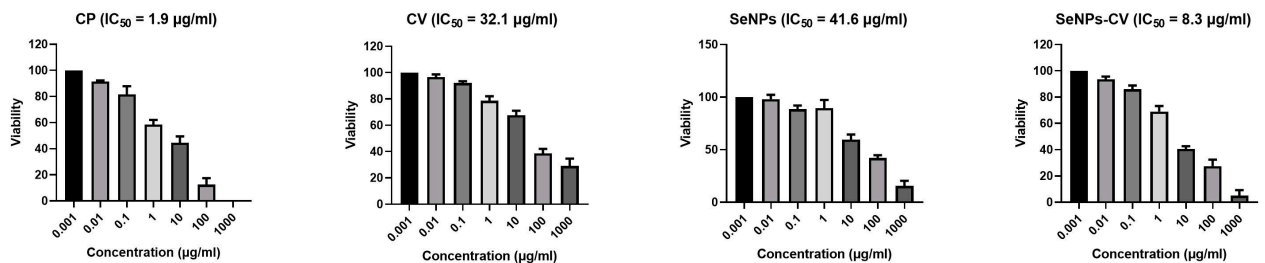


Figure 2. Effects of different concentrations of cisplatin (CP), carvacrol (CV), metal nanoparticles of selenium (SeNPs), and green-synthesized SeNPs (SeNPs-CV) using CV on MCF-7 cells with the viability measured with an MTT assay. Values represent the mean of three experiments \pm standard deviation (SD).

3.3. SeNPs-CV Treatment-Induced Apoptosis in MCF-7 Cells

As seen in Figure 3, after 24 h, all treatment groups had a substantially greater percentage of early and late apoptotic cells than the vehicle group ($p < 0.05$). In contrast to the CV group, SeNPs-CV substantially enhanced the proportion of early and late apoptotic cells ($p < 0.05$). Moreover, there was no discernible distinction in the apoptotic impact between the SeNP-CV and CP groups.

Consistent with these results, MCF-7 cells treated with CP or SeNPs-CV revealed significant increases ($p < 0.05$) in the levels of apoptotic markers (Bax, caspase-3, and cytochrome c) and a significant decrease ($p < 0.05$) in the levels of the anti-apoptotic protein Bcl-2 as compared to both the CV and vehicle groups ($p < 0.05$). Meanwhile, administration of CV alone increased cytochrome c levels notably as compared to the vehicle group ($p < 0.05$; Figure 4).

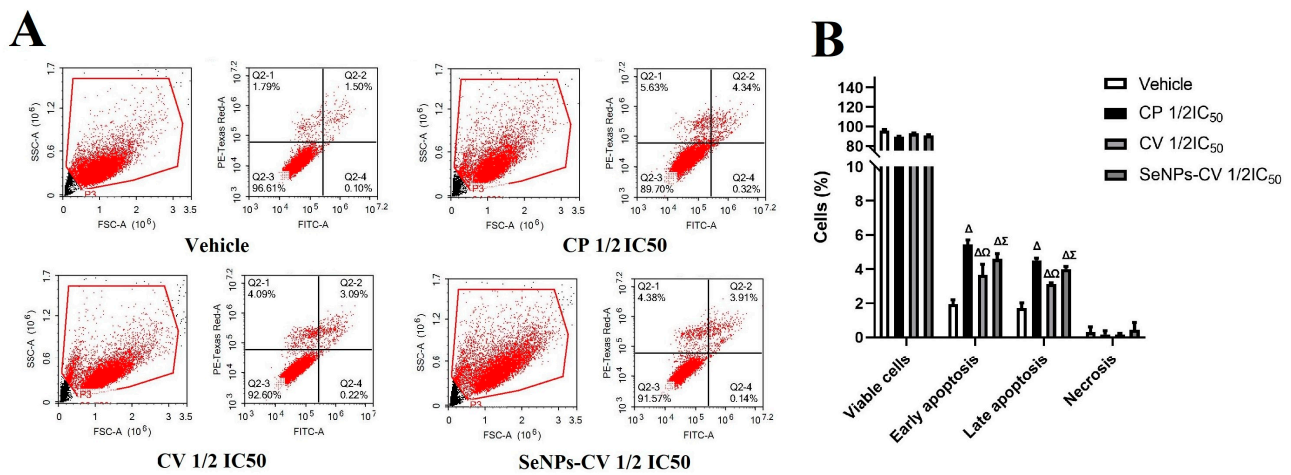


Figure 3. Induction effect of cell apoptosis by cisplatin (CP), carvacrol (CV), or green-synthesized SeNPs (SeNPs-CV) on MCF-7 cells. **(A)** Annexin V-PI co-staining assay to assess apoptosis in MCF-7 cells. **(B)** Percent of apoptotic cells. Values represent the mean of three experiments \pm standard deviation (SD). Δ denotes significance with respect to the untreated control cells ($p < 0.05$). Ω denotes significance with respect to the CP-treated cells ($p < 0.05$). Σ denotes significance with respect to the CV-treated cells ($p < 0.05$).

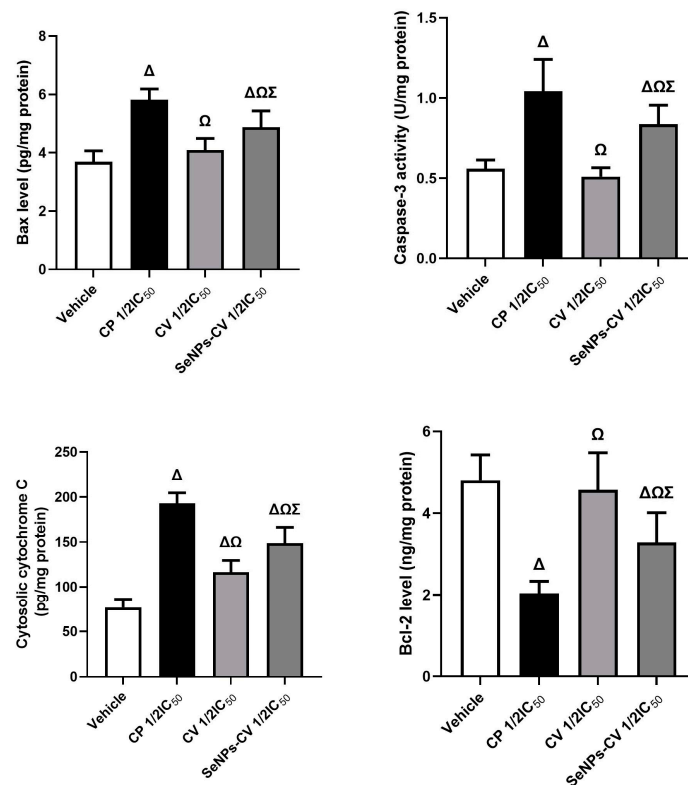


Figure 4. Cisplatin (CP), carvacrol (CV), or green-synthesized SeNPs (SeNPs-CV) enhanced cell apoptosis on MCF-7 cells detected by measuring pro-apoptotic (Bax, caspase-3, and cytochrome c) and anti-apoptotic (Bcl-2) markers. Values represent the mean of three experiments \pm standard deviation (SD). Δ denotes significance with respect to the untreated control cells ($p < 0.05$). Ω denotes significance with respect to the CP-treated cells ($p < 0.05$). Σ denotes significance with respect to the CV-treated cells ($p < 0.05$).

3.4. Effect of SeNPs-CV in the Expression Rate of Proliferating Cell Nuclear Antigen (PCNA)

As indicated in Figure 5, a remarkable downregulation ($p < 0.05$) in the expression rate of the PCNA gene was observed in the CP, CV, and SeNP-CV groups compared to the vehicle group. Meanwhile, there was a significant decline in the level of PCNA mRNA expression in the CP group compared to the CV and SeNPs-CV groups ($p < 0.05$), but no significant difference was observed between the CV and SeNPs-CV groups.

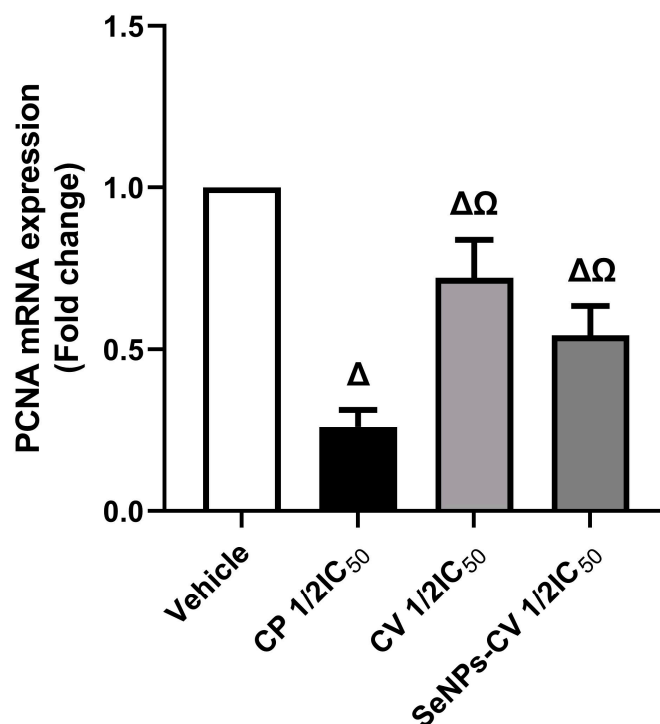


Figure 5. Cisplatin (CP), carvacrol (CV), or green-synthesized SeNPs (SeNPs-CV) suppressed MCF-7 cell proliferation detected by measuring the mRNA expression rate of proliferating cell nuclear antigen (PCNA). Values represent the mean of three experiments \pm standard deviation (SD). Δ denotes significance with respect to the untreated control cells ($p < 0.05$). Ω denotes significance with respect to the CP-treated cells ($p < 0.05$).

3.5. SeNPs-CV Treatment Enhanced the Oxidative Stress in MCF-7 Cells

ROS production and antioxidant exhaustion are fundamental mechanisms underlying the apoptotic impact of anticancer medicines on tumor cells. Therefore, 8-OHDG, NO, ROS, and LPO levels were evaluated as oxidant biomarkers, whereas GSH levels and antioxidant enzymes' (SOD, CAT, and GPx) activities were determined as antioxidant biomarkers. As shown in Figure 6, considerable rises were observed in 8-OHDG, ROS, NO, and LPO, paralleled by a significant drop in GSH level and antioxidant enzymes activity in the CP and SeNPs-CV groups compared with the vehicle group ($p < 0.05$). However, LPO levels were significantly higher in the CV group than in the vehicle group ($p < 0.05$). Meanwhile, compared to CP-treated cells, cells treated with CV displayed markedly ($p < 0.05$) higher levels of antioxidants and lower levels of oxidative stress markers. Overall, the oxidative effect of SeNPs-CV was stronger in MCF-7 cells than that of CV alone.

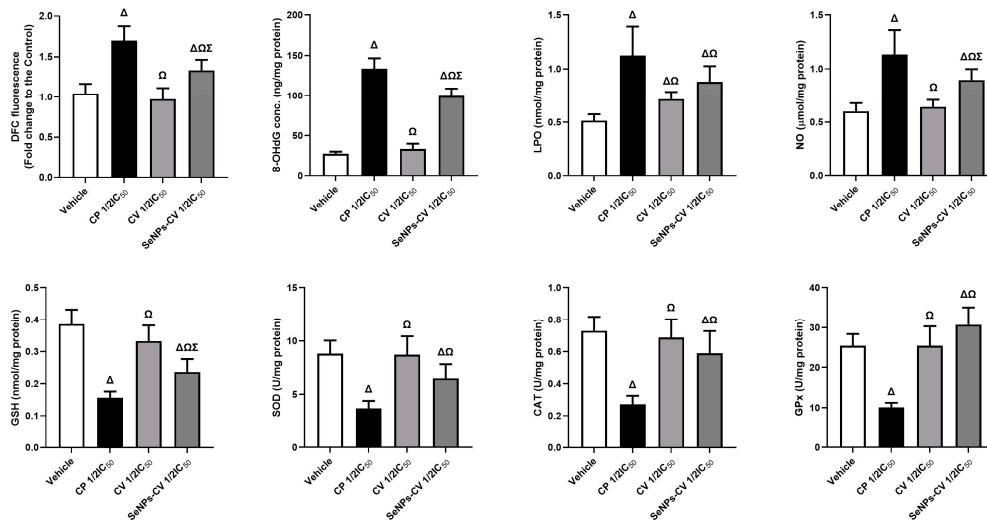


Figure 6. Cisplatin (CP), carvacrol (CV), or green-synthesized SeNPs (SeNPs-CV) induced oxidative stress on MCF-7 cells detected by measuring oxidants (ROS, 8-OHDG, LPO, and NO) and antioxidants (GSH, SOD, CAT, and GPx) markers. Values represent the mean of three experiments \pm standard deviation (SD). Δ denotes significance with respect to the untreated control cells ($p < 0.05$). Ω denotes significance with respect to the CP-treated cells ($p < 0.05$). Σ denotes significance with respect to the CV-treated cells ($p < 0.05$).

3.6. SeNPs-CV Stimulated IL-1 β Production

The levels of IL-1 β were evaluated to assess the effect of SeNPs-CV on the inflammatory cascade in MCF-7 cells. A marked increase ($p < 0.05$) was noted in the inflammatory marker IL-1 β in cells subjected to CP and SeNPs-CV compared to the vehicle group. Furthermore, MCF-7 cells treated with SeNPs-CV showed notable increases ($p < 0.05$) in IL-1 β levels as compared to the CV group (Figure 7).

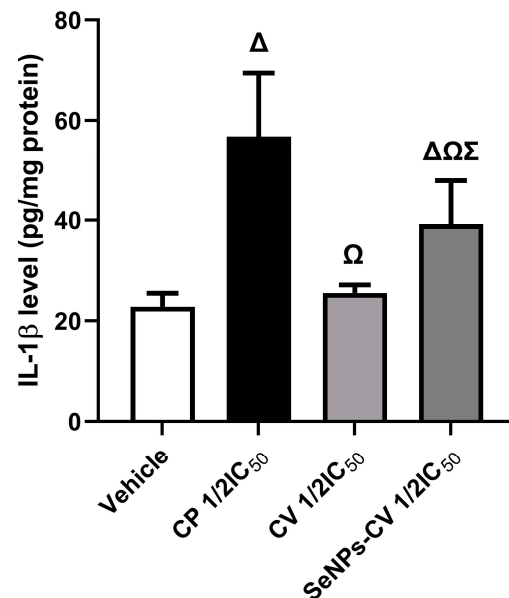


Figure 7. Cisplatin (CP), carvacrol (CV), or green-synthesized SeNPs (SeNPs-CV) enhanced inflammatory cascade on MCF-7 cells detected by measuring the mRNA expression rate of interleukin-1 beta (IL-1 β). Values represent the mean of three experiments \pm standard deviation (SD). Δ denotes significance with respect to the untreated control cells ($p < 0.05$). Ω denotes significance with respect to the CP-treated cells ($p < 0.05$). Σ denotes significance with respect to the CV-treated cells ($p < 0.05$).

4. Discussion

Due to the high death rate associated with BC and the limitations of standard therapies, it is vital to develop innovative methods for treating this illness [27]. The anticancer properties of the natural plant extract CV in several cancer types have recently been assessed. CV's limited solubility and bioavailability, however, may limit its anti-cancer effect [28,29]. Combination therapy using nanotechnology is currently a compelling argument for cancer therapy because of its greater efficacy and fewer adverse effects. In this regard, this study postulated that SeNPs green-synthesized using CV would synergize and increase the anticancer effect of CV.

In the current study, the cytotoxic activities of CP, CV, SeNPs, and SeNPs-CV were evaluated in MCF-7 cells. The IC_{50} of CP was found to be 1.9 $\mu\text{g}/\text{mL}$, while the IC_{50} of CV and SeNPs alone was 32.1 $\mu\text{g}/\text{mL}$ and 41.6 $\mu\text{g}/\text{mL}$, respectively, whereas the IC_{50} of the SeNPs-CV was 8.3 $\mu\text{g}/\text{mL}$, approximately four times lower than that of CV, indicating a synergetic potential between CV and SeNPs. These results also indicated the marked cytotoxic effects of CV and SeNPs-CV in MCF-7 cell lines. Additionally, the study's findings revealed that cells exposed to either CV or SeNPs-CV had a much higher percentage of cells in the early and late phases of apoptosis as contrasted to the vehicle cells, as shown in Figure 3.

These results are in line with those of previous studies that have confirmed the anti-proliferative effects of CV in many types of cancer cell lines [30,31]. Moreover, CV dramatically increased apoptosis in several BC cell lines, with MDA-MB-231 cells being the most susceptible and MCF-7 cells being the least sensitive, suggesting that the efficacy of CV may vary depending on the type of BC [5].

Numerous studies have confirmed that green-synthesized SeNPs are highly effective in the treatment of various forms of cancer [32,33]. In a recent study, SeNPs showed stronger anti-proliferative activities in MCF-7 cells, with an IC_{50} value of 25 μg . Similarly, Soltani and Darbemamieh [34] reported that SeNPs decreased MCF-7 cell proliferation in a dose-dependent manner owing to their cytotoxicity and apoptotic potential.

One of the most intriguing findings of this study was that the conjugation of CV with SeNPs led to an increase in anti-proliferative and anti-apoptotic effects when compared with CV alone, as evidenced by the decrease in IC_{50} to 8.3 $\mu\text{g}/\text{mL}$. Our results also revealed a marked elevation in the percentage of apoptotic cells in the SeNPs-CV group in contrast to that in the CV group. These findings agree with those of a previous report [1], in which the coupling of SeNPs with the natural flavonoid apigenin demonstrated significantly greater cytotoxic potential in BC therapy than either component alone. In another study, conjugation of SeNPs with berberine, a natural alkaloid extract, demonstrated greater cytotoxic efficacy than that of each agent alone [32].

Due to their propensity to induce apoptosis and autophagy, reactive oxygen species (ROS) have recently received interest for their therapeutic utility. Previous studies have revealed that ROS may chemically bind to nucleic acids and proteins by interacting with the nucleophilic center of the cell, which can damage DNA. To enhance clinical outcomes for cancer patients, novel methods that increase ROS levels have been included in cancer therapy [5]. The formation of ROS in cells is modulated by a number of anticancer drugs by triggering various regulatory systems. For instance, doxorubicin increases ROS production by causing electron leakage and the Fenton reaction, whereas gamitrinib boosts ROS generation by causing malignant cells' mitochondria to collapse [16]. Moreover, the identification of intracellular ROS generation is a key marker for early cellular reactions with NPs and the initial step in the cytotoxicity cascade. However, when NPs generated sufficient intracellular ROS, cells stopped carrying out their typical functions, ultimately leading to cell death [35].

The findings of this study revealed significant inductions of oxidative stress markers, such as ROS, 8-OHdG, LPO, and NO, accompanied by a drop in the antioxidant markers (CAT, SOD, and GPx activities and GSH levels) in MCF-7 cells exposed to SeNPs-CV in contrast to the control cells. These observations indicated that SeNPs-CV increased

oxidative stress in MCF-7 cells. However, at a dose of 16 $\mu\text{g}/\text{mL}$ (half the IC_{50}), CV alone had little effect on the oxidant/antioxidant system and only affected LPO levels, whereas conjugation with SeNPs boosted its oxidative effect. GSH contents might indicate a cell's antioxidant capability, as GSH protects enzyme thiol groups and interacts with free radicals. Here, the depletion of GSH contents after SeNPs-CV administration reflects the cytotoxicity of synthesized SeNPs-CV.

These findings were in line with Lim et al. [36], who concluded that CV induced notable ROS production, as indicated by an increase in LPO and 8-OHdG in tumor cells. Similarly, it was found that CV acts as a prooxidant and promotes cytotoxicity in human epithelial colorectal cancer [37]. On the other hand, the therapeutic use of SeNPs has drawn the most attention in cancer therapy because tumor cells are more susceptible to oxidative stress triggered by elevated Se levels than normal cells. Moreover, SeNPs may cause ROS-mediated cell death when they aggregate in cancerous cells, while providing anti-oxidation and cancer prevention in healthy tissues at low quantities [38].

Oxidative stress and inflammation can initiate the apoptotic signaling pathway as a result of mitochondrial dysfunction. When the integrity of the mitochondrial membrane is disrupted, cytochrome c moves from the mitochondria to the cytosol. This starts the caspase signaling cascade, which damages the DNA [15]. In addition, ROS controls the translocation, phosphorylation, and cleavage of the pro-apoptotic Bcl-2 protein, which induces apoptosis [1].

In the current study, increases in apoptotic markers (caspase-3, Bax, and cytochrome c) and reductions in the anti-apoptotic protein Bcl-2 were seen in MCF-7 cells treated with SeNPs-CV. These changes in apoptotic markers were in line with a rise in the number of cells that started early or late apoptosis after being exposed to SeNPs-CV, as shown in Figure 3. These results were in harmony with former studies [36,39], which stated that CV's anti-proliferative effects on metastatic BC cells were based on the typical apoptotic response, which includes a drop in mitochondrial membrane potential and a rise in cytochrome c discharge from mitochondria, a decline in the Bcl-2/Bax ratio, an elevation in caspase activity, PARP cleavage, and DNA fragmentation. In the same context, CV has also been observed to cause mitochondrial apoptosis in human oral squamous cell cancer [40], leukemia and lymphoma cells [13], and colon cancer cells [28] by disrupting matrix metalloproteinases (MMPs) and altering the expression rates of Bax/Bcl2 proteins.

Our findings demonstrated that SeNPs-CV were more efficient in inducing apoptotic markers compared with CV alone, indicating the synergistic effect of SeNPs. Formerly, Se has been shown to stimulate apoptosis in cancerous cells through ROS production, activation of several caspases, and the formation of apoptotic bodies [41]. Furthermore, Ferro et al. [42] stated that SeNPs increase the expression of Bax and cytochrome c in MCF-7 cells. IL-1 β has been shown in several studies to have a substantial pro-apoptotic impact in human cells by boosting the expression ratio of Bax/Bcl-2, releasing cytochrome c from the mitochondria, and stimulating caspase-9 and caspase-3 to accomplish the apoptotic process. Subsequently, mitochondrial damage was detected following IL-1 β stimulation [43]. In the current study, administration of CV or SeNPs-CV increased the levels of IL-1 β in MCF-7 cells. These findings proved that SeNPs-CV or CV might stimulate apoptosis in MCF-7 cells through the activation of IL-1 β synthesis. This increment in IL-1 β may be due to the oxidative effect of CV and SeNPs-CV, where a crosstalk between oxidative stress and inflammation has been demonstrated, as ROS trigger the activation of NF- κB , which in turn regulates the production of several inflammatory mediators, including IL-1 β [44]. These findings are consistent with prior studies showing that IL-1 β promotes apoptosis in pancreatic RIm5F cells via stimulating nitric oxide generation [45] and ceramide synthesis in EL4 thymoma cells [46]. Additionally, Shen et al. [43] indicated that endogenously produced mature IL-1 β is directly involved in cell death through the activation of the IL-1 β converting enzyme (ICE), which plays a direct role in mediating the apoptotic cascade.

Proliferating cell nuclear antigen (PCNA) is termed the “ringmaster of the genome” as it regulates the cell cycle and participates in DNA synthesis. So, it is strongly related to prognosis and survival in most types of solid malignancies, such as BC, suggesting an active role of PCNA in tumorigenesis [47]. As a result, PCNA is widely utilized as a marker of cell proliferation in both healthy and malignant tissues since it generally represents cell proliferation activity [48]. Similarly, Jurková et al. [49] discovered that PCNA protein levels were higher in BC patients in clinical stages III–IV and lymph node metastasis. Interestingly, in the present study, the administration of CV or SeNPs-CV considerably reduced PCNA expression rates in MCF-7 cells. These findings clearly show the role of CV and SeNPs-CV in the inhibition of tumorigenesis and proliferation in BC through the inhibition of PCNA gene expression. In agreement with our findings, Se treatment arrested BC cell lines in the G1 phase of the cell cycle and inhibited the expression of PCNA genes while inducing the expressions of certain caspase genes [50]. On the other hand, supplementation with CV had an antimetastatic impact on liver cancer by drastically lowering PCNA expression and preventing the local spread of cancerous cells [51]. Further supporting the advantages of SeNPs-CV versus CV, our results demonstrated a significant decrease in PCNA expression rates in the combination group compared to the only-CV group.

5. Conclusions

We can conclude that the conjugation of SeNPs with CV results in the synergistic therapeutic effectiveness and substantial suppression of MCF-7 cell proliferation. The combination of SeNPs and CV can suppress breast cancer by inducing oxidative stress, inflammation, and apoptosis in BC cells. The mechanism of action of SeNPs-CV may be linked to signaling pathways including caspase-3, Bax/BCI-2, IL-1 β , and PCNA. In this regard, the current findings provide a unique concept of using SeNPs-CV as a powerful breast cancer therapy.

Author Contributions: Conceptualization, M.S.O., S.M.A. and M.M.H.; methodology, M.M.H.; validation, A.E.A.M.; formal analysis, M.S.O. and M.M.H.; investigation, M.M.H.; resources, S.M.A.; writing—original draft preparation, M.S.O. and O.A.H.; writing—review and editing, M.M.H. and A.E.A.M.; visualization, supervision, and project administration, M.S.O.; funding acquisition, M.S.O. and S.M.A. All authors have read and agreed to the published version of the manuscript.

Funding: This research has been funded by the Engineer Abdullah Bugshan Chair for Breast Cancer Research at the University of Ha’il, Saudi Arabia, through project number SCR-22092.

Institutional Review Board Statement: Not applicable.

Informed Consent Statement: Not applicable.

Data Availability Statement: All relevant data are within the paper.

Acknowledgments: This research has been funded by the Engineer Abdullah Bugshan Chair for Breast Cancer Research at the University of Ha’il, Saudi Arabia, through project number (SCR-22092).

Conflicts of Interest: The authors declare no conflict of interest.

References

1. Al-Otaibi, A.M.; Al-Gebaly, A.S.; Almeer, R.; Albasher, G.; Al-Qahtani, W.S.; Abdel Moneim, A.E. Potential of green-synthesized selenium nanoparticles using apigenin in human breast cancer MCF-7 cells. *Environ. Sci. Pollut. Res. Int.* **2022**, *29*, 47539–47548. [[CrossRef](#)] [[PubMed](#)]
2. Othman, M.; Obeidat, S.; Al-Bagawi, A.; Fareid, M.; El-Borady, O.; Kassab, R.; Abdel Moneim, A. Evaluation of the Potential Role of Silver Nanoparticles Loaded with Berberine in Improving Anti-Tumor Efficiency. *Pharm. Sci.* **2022**, *28*, 86–93. [[CrossRef](#)]
3. Othman, M.S.; Obeidat, S.T.; Aleid, G.M.; Al-Bagawi, A.H.; Fareid, M.A.; Hameed, R.A.; Mohamed, K.M.; Abdelfattah, M.S.; Fehaid, A.; Hussein, M.M.; et al. Green Synthesized Selenium Nanoparticles Using Syzygium aromaticum (Clove) Extract Reduce Pentylene-tetrazol-Induced Epilepsy and Associated Cortical Damage in Rats. *Appl. Sci.* **2023**, *13*, 1050. [[CrossRef](#)]
4. Mohamed, K.M.; Abdelfattah, M.S.; El-khadragy, M.; Al-Megrin, W.A.; Fehaid, A.; Kassab, R.B.; Abdel Moneim, A.E. Rutin-loaded selenium nanoparticles modulated the redox status, inflammatory, and apoptotic pathways associated with pentylene-tetrazole-induced epilepsy in mice. *Green. Process. Synth.* **2023**, *12*, 20230010. [[CrossRef](#)]

5. Li, L.; He, L.; Wu, Y.; Zhang, Y. Carvacrol affects breast cancer cells through TRPM7 mediated cell cycle regulation. *Life Sci.* **2021**, *266*, 118894. [[CrossRef](#)]
6. Carqueijeiro, I.; Langley, C.; Grzech, D.; Koudounas, K.; Papon, N.; O'Connor, S.E.; Courdavault, V. Beyond the semi-synthetic artemisinin: Metabolic engineering of plant-derived anti-cancer drugs. *Curr. Opin. Biotechnol.* **2020**, *65*, 17–24. [[CrossRef](#)]
7. Masyita, A.; Mustika Sari, R.; Dwi Astuti, A.; Yasir, B.; Rahma Rumata, N.; Emran, T.B.; Nainu, F.; Simal-Gandara, J. Terpenes and terpenoids as main bioactive compounds of essential oils, their roles in human health and potential application as natural food preservatives. *Food Chem. X* **2022**, *13*, 100217. [[CrossRef](#)]
8. Suntres, Z.E.; Coccimiglio, J.; Alipour, M. The bioactivity and toxicological actions of carvacrol. *Crit. Rev. Food Sci. Nutr.* **2015**, *55*, 304–318. [[CrossRef](#)]
9. De Vincenzi, M.; Stammati, A.; De Vincenzi, A.; Silano, M. Constituents of aromatic plants: Carvacrol. *Fitoterapia* **2004**, *75*, 801–804. [[CrossRef](#)]
10. Javed, H.; Meeran, M.F.N.; Jha, N.K.; Ojha, S. Carvacrol, a Plant Metabolite Targeting Viral Protease (M(pro)) and ACE2 in Host Cells Can Be a Possible Candidate for COVID-19. *Front. Plant. Sci.* **2020**, *11*, 601335. [[CrossRef](#)]
11. Elbe, H.; Yigitturk, G.; Cavusoglu, T.; Baygar, T.; Ozgul Onal, M.; Ozturk, F. Comparison of ultrastructural changes and the anticarcinogenic effects of thymol and carvacrol on ovarian cancer cells: Which is more effective? *Ultrastruct. Pathol.* **2020**, *44*, 193–202. [[CrossRef](#)]
12. Mastelic, J.; Jerkovic, I.; Blazevic, I.; Poljak-Blazi, M.; Borovic, S.; Ivancic-Bace, I.; Smrecki, V.; Zarkovic, N.; Brcic-Kostic, K.; Vikić-Topić, D.; et al. Comparative study on the antioxidant and biological activities of carvacrol, thymol, and eugenol derivatives. *J. Agric. Food Chem.* **2008**, *56*, 3989–3996. [[CrossRef](#)]
13. Sampaio, L.A.; Pina, L.T.S.; Serafini, M.R.; Tavares, D.D.S.; Guimaraes, A.G. Antitumor Effects of Carvacrol and Thymol: A Systematic Review. *Front. Pharmacol.* **2021**, *12*, 702487. [[CrossRef](#)]
14. Chen, G.; Yang, F.; Fan, S.; Jin, H.; Liao, K.; Li, X.; Liu, G.B.; Liang, J.; Zhang, J.; Xu, J.F.; et al. Immunomodulatory roles of selenium nanoparticles: Novel arts for potential immunotherapy strategy development. *Front. Immunol.* **2022**, *13*, 956181. [[CrossRef](#)]
15. Al-Brakati, A.; Alsharif, K.F.; Alzahrani, K.J.; Kabrah, S.; Al-Amer, O.; Oyouni, A.A.; Habotta, O.A.; Lokman, M.S.; Bauomy, A.A.; Kassab, R.B. Using green biosynthesized lycopene-coated selenium nanoparticles to rescue renal damage in glycerol-induced acute kidney injury in rats. *Int. J. Nanomed.* **2021**, *16*, 4335. [[CrossRef](#)]
16. Khan, A.Q.; Rashid, K.; AlAmodi, A.A.; Agha, M.V.; Akhtar, S.; Hakeem, I.; Raza, S.S.; Uddin, S. Reactive oxygen species (ROS) in cancer pathogenesis and therapy: An update on the role of ROS in anticancer action of benzophenanthridine alkaloids. *Biomed. Pharm.* **2021**, *143*, 112142. [[CrossRef](#)]
17. Dkhil, M.A.; Zrieq, R.; Al-Quraishy, S.; Abdel Moneim, A.E. Selenium Nanoparticles Attenuate Oxidative Stress and Testicular Damage in Streptozotocin-Induced Diabetic Rats. *Molecules* **2016**, *21*, 1517. [[CrossRef](#)]
18. van Meerloo, J.; Kaspers, G.J.; Cloos, J. Cell sensitivity assays: The MTT assay. *Methods Mol. Biol.* **2011**, *731*, 237–245. [[CrossRef](#)]
19. Othman, M.S.; Al-Bagawi, A.H.; Obeidat, S.T.; Fareid, M.A.; Habotta, O.A.; Moneim, A.E.A. Antitumor activity of zinc nanoparticles synthesized with berberine on human epithelial colorectal adenocarcinoma (Caco-2) cells through acting on Cox-2/NF-κB and p53 pathways. *Anticancer Agents Med. Chem.* **2021**, *22*, 2002–2010. [[CrossRef](#)]
20. Ohkawa, H.; Ohishi, N.; Yagi, K. Assay for lipid peroxides in animal tissues by thiobarbituric acid reaction. *Anal. Biochem.* **1979**, *95*, 351–358. [[CrossRef](#)]
21. Green, L.C.; Wagner, D.A.; Glogowski, J.; Skipper, P.L.; Wishnok, J.S.; Tannenbaum, S.R. Analysis of nitrate, nitrite, and [15N]nitrate in biological fluids. *Anal. Biochem.* **1982**, *126*, 131–138. [[CrossRef](#)]
22. Aebi, H. Catalase in vitro. *Methods Enzymol.* **1984**, *105*, 121–126. [[PubMed](#)]
23. Misra, H.P.; Fridovich, I. The role of superoxide anion in the autoxidation of epinephrine and a simple assay for superoxide dismutase. *J. Biol. Chem.* **1972**, *247*, 3170–3175. [[CrossRef](#)] [[PubMed](#)]
24. Tappel, A.L. Glutathione peroxidase and hydroperoxides. *Methods Enzymol.* **1978**, *52*, 506–513. [[CrossRef](#)] [[PubMed](#)]
25. Akerboom, T.P.; Sies, H. Assay of glutathione, glutathione disulfide, and glutathione mixed disulfides in biological samples. *Methods Enzymol.* **1981**, *77*, 373–382. [[CrossRef](#)]
26. Shahabadi, N.; Zendehecheshm, S.; Khademi, F. Selenium nanoparticles: Synthesis, in-vitro cytotoxicity, antioxidant activity and interaction studies with ct-DNA and HSA, Hb and Cyt c serum proteins. *Biotechnol. Rep.* **2021**, *30*, e00615. [[CrossRef](#)]
27. El-Naa, M.M.; Othman, M.; Younes, S. Sildenafil potentiates the antitumor activity of cisplatin by induction of apoptosis and inhibition of proliferation and angiogenesis. *Drug Des. Dev. Ther.* **2016**, *10*, 3661–3672. [[CrossRef](#)]
28. Fan, K.; Li, X.; Cao, Y.; Qi, H.; Li, L.; Zhang, Q.; Sun, H. Carvacrol inhibits proliferation and induces apoptosis in human colon cancer cells. *Anti-Cancer Drugs* **2015**, *26*, 813–823. [[CrossRef](#)]
29. Luo, Y.; Wu, J.Y.; Lu, M.H.; Shi, Z.; Na, N.; Di, J.M. Carvacrol Alleviates Prostate Cancer Cell Proliferation, Migration, and Invasion through Regulation of PI3K/Akt and MAPK Signaling Pathways. *Oxid. Med. Cell Longev.* **2016**, *2016*, 1469693. [[CrossRef](#)]
30. Koparal, A.T.; Zeytinoglu, M. Effects of Carvacrol on a Human Non-Small Cell Lung Cancer (NSCLC) Cell Line, A549. *Cytotechnology* **2003**, *43*, 149–154. [[CrossRef](#)]
31. Melusova, M.; Jantova, S.; Horvathova, E. Carvacrol and rosemary oil at higher concentrations induce apoptosis in human hepatoma HepG2 cells. *Interdiscip. Toxicol.* **2014**, *7*, 189–194. [[CrossRef](#)]
32. Othman, M.S.; Obeidat, S.T.; Al-Bagawi, A.H.; Fareid, M.A.; Fehaid, A.; Moneim, A.E.A. Green-synthesized selenium nanoparticles using berberine as a promising anticancer agent. *J. Integr. Med.* **2022**, *20*, 65–72. [[CrossRef](#)]

33. Spyridopoulou, K.; Aindelis, G.; Pappa, A.; Chlichlia, K. Anticancer Activity of Biogenic Selenium Nanoparticles: Apoptotic and Immunogenic Cell Death Markers in Colon Cancer Cells. *Cancers* **2021**, *13*, 5335. [[CrossRef](#)]
34. Soltani, L.; Darbemamieh, M. Anti-proliferative, apoptotic potential of synthesized selenium nanoparticles against breast cancer cell line (MCF7). *Nucleosides Nucleotides Nucleic Acids* **2021**, *40*, 926–941. [[CrossRef](#)]
35. Yu, Z.; Li, Q.; Wang, J.; Yu, Y.; Wang, Y.; Zhou, Q.; Li, P. Reactive Oxygen Species-Related Nanoparticle Toxicity in the Biomedical Field. *Nanoscale Res. Lett.* **2020**, *15*, 115. [[CrossRef](#)]
36. Lim, W.; Ham, J.; Bazer, F.W.; Song, G. Carvacrol induces mitochondria-mediated apoptosis via disruption of calcium homeostasis in human choriocarcinoma cells. *J. Cell Physiol.* **2019**, *234*, 1803–1815. [[CrossRef](#)]
37. Llana-Ruiz-Cabello, M.; Gutiérrez-Praena, D.; Pichardo, S.; Moreno, F.J.; Bermúdez, J.M.; Aucejo, S.; Cameán, A.M. Cytotoxicity and morphological effects induced by carvacrol and thymol on the human cell line Caco-2. *Food Chem. Toxicol.* **2014**, *64*, 281–290. [[CrossRef](#)]
38. Zhuang, Y.; Li, L.; Feng, L.; Wang, S.; Su, H.; Liu, H.; Liu, H.; Wu, Y. Mitochondrion-targeted selenium nanoparticles enhance reactive oxygen species-mediated cell death. *Nanoscale* **2020**, *12*, 1389–1396. [[CrossRef](#)]
39. Moradipour, A.; Dariushnejad, H.; Ahmadizadeh, C.; Lashgarian, H.E. Dietary flavonoid carvacrol triggers the apoptosis of human breast cancer MCF-7 cells via the p53/Bax/Bcl-2 axis. *Med. Oncol.* **2022**, *40*, 46. [[CrossRef](#)]
40. Dai, W.; Sun, C.; Huang, S.; Zhou, Q. Carvacrol suppresses proliferation and invasion in human oral squamous cell carcinoma. *Onco. Targets. Ther.* **2016**, *9*, 2297–2304. [[CrossRef](#)]
41. Kirwale, S.; Pooladanda, V.; Thatikonda, S.; Murugappan, S.; Khurana, A.; Godugu, C. Selenium nanoparticles induce autophagy mediated cell death in human keratinocytes. *Nanomedicine* **2019**, *14*, 1991–2010. [[CrossRef](#)] [[PubMed](#)]
42. Ferro, C.; Florindo, H.F.; Santos, H.A. Selenium Nanoparticles for Biomedical Applications: From Development and Characterization to Therapeutics. *Adv. Healthc. Mater.* **2021**, *10*, e2100598. [[CrossRef](#)] [[PubMed](#)]
43. Shen, J.; Xu, S.; Zhou, H.; Liu, H.; Jiang, W.; Hao, J.; Hu, Z. IL-1 β induces apoptosis and autophagy via mitochondria pathway in human degenerative nucleus pulposus cells. *Sci. Rep.* **2017**, *7*, 41067. [[CrossRef](#)] [[PubMed](#)]
44. Sun, D.; Sun, C.; Qiu, G.; Yao, L.; Yu, J.; Al Sberi, H.; Fouda, M.S.; Othman, M.S.; Lokman, M.S.; Kassab, R.B.; et al. Allicin mitigates hepatic injury following cyclophosphamide administration via activation of Nrf2/ARE pathways and through inhibition of inflammatory and apoptotic machinery. *Environ. Sci. Pollut. Res. Int.* **2021**, *28*, 39625–39636. [[CrossRef](#)]
45. Ankarcona, M.; Dypbukt, J.M.; Brüne, B.; Nicotera, P. Interleukin-1 beta-induced nitric oxide production activates apoptosis in pancreatic RINm5F cells. *Exp. Cell Res.* **1994**, *213*, 172–177. [[CrossRef](#)]
46. Mathias, S.; Younes, A.; Kan, C.C.; Orlow, I.; Joseph, C.; Kolesnick, R.N. Activation of the sphingomyelin signaling pathway in intact EL4 cells and in a cell-free system by IL-1 beta. *Science* **1993**, *259*, 519–522. [[CrossRef](#)]
47. Stoimenov, I.; Helleday, T. PCNA on the crossroad of cancer. *Biochem. Soc. Trans.* **2009**, *37*, 605–613. [[CrossRef](#)]
48. Lu, E.M.; Ratnayake, J.; Rich, A.M. Assessment of proliferating cell nuclear antigen (PCNA) expression at the invading front of oral squamous cell carcinoma. *BMC Oral. Health* **2019**, *19*, 233. [[CrossRef](#)]
49. Jurikova, M.; Danihel, L.; Polak, S.; Varga, I. Ki67, PCNA, and MCM proteins: Markers of proliferation in the diagnosis of breast cancer. *Acta Histochem.* **2016**, *118*, 544–552. [[CrossRef](#)]
50. El-Bayoumy, K.; Sinha, R. Molecular chemoprevention by selenium: A genomic approach. *Mutat. Res.* **2005**, *591*, 224–236. [[CrossRef](#)]
51. Subramanian, J.; Krishnan, G.; Balan, R.; Mgi, D.; Ramasamy, E.; Ramalingam, S.; Veerabathiran, R.; Thandavamoorthy, P.; Mani, G.K.; Thiruvengadam, D. Carvacrol modulates instability of xenobiotic metabolizing enzymes and downregulates the expressions of PCNA, MMP-2, and MMP-9 during diethylnitrosamine-induced hepatocarcinogenesis in rats. *Mol. Cell Biochem.* **2014**, *395*, 65–76. [[CrossRef](#)]

Disclaimer/Publisher’s Note: The statements, opinions and data contained in all publications are solely those of the individual author(s) and contributor(s) and not of MDPI and/or the editor(s). MDPI and/or the editor(s) disclaim responsibility for any injury to people or property resulting from any ideas, methods, instructions or products referred to in the content.